Proc. Natl. Acad. Sci. USA
Vol. 77, No. 10, pp. 5626–5629, October 1980
Physics

Soliton dynamics in polyacetylene

(electron–phonon interaction/broken symmetry ground state/nonlinear dynamics of quantum fields)

W. P. SU* AND J. R. SCHRIEFFER

Department of Physics, University of California, Santa Barbara, California 93106

Contributed by J. Robert Schrieffer, June 30, 1980

ABSTRACT **The equations of motion of the coupled electron–phonon system are integrated in real time for the model of polyacetylene recently proposed. To illustrate the physical behavior of this nonlinear system we consider the time evolution starting from three physically relevant configurations: (*i*) end generated soliton, (*ii*) electron–hole pair generation of a charged soliton–antisoliton pair, and (*iii*) the dressing of an injected electron. The calculations show that the system relaxes within a time of order 10^{-13} sec, converting excited electron–hole pairs into soliton–antisoliton pairs.**

Polyacetylene $(CH)_x$ is a simple linear polymer formed as a chain of CH groups. The *trans* configuration, corresponding to a herringbone structure of CH groups, is the stable phase at room temperature and below. Because undoped $(CH)_x$ has exactly one π electron per CH group, the traditional view is that the ground state exhibits a lattice distortion or dimerization in which bond lengths between CH groups are alternately longer and shorter than the average bond length a (Fig. 1). In the language of condensed matter physics, *trans* $(CH)_x$ has undergone a commensurate Peierls distortion of index 2. The doubling of the size of the unit cell introduces a periodic potential acting on the π electrons which opens a gap 2Δ in the π energy band structure at the Fermi surface, converting the one-dimensional metal into a semiconductor (1), as is observed.

However, evidence is growing (2–4) that, instead of the familiar electron and hole excitations characteristic of a conventional semiconductor, the stable low-energy charge-carrying excitations in $(CH)_x$ are charged solitons, $S^{\pm}$. These excitations are in essence charged domain walls (2, 3, 5) separating regions with different ground state order as illustrated in Fig. 1. The A and B ground states are related by interchanging double and single (short and long) bonds. As Su *et al.* (2, 3) have shown, S^+ and S^- have zero spin in contrast with holes and electrons which have spin ½. Also, the neutral soliton S^0 has spin ½. The width of the soliton is approximately 14 lattice spacings for $(CH)_x$ and its mass is remarkably small, roughly six electron masses. There is considerable experimental evidence supporting these results.

In order to gain further insight into dynamical processes in $(CH)_x$, such as electrical conductivity, spin diffusion, optical absorption, photoconductivity, etc., we have carried out a real-time integration of the equations of motion describing the coupled electron and phonon fields. Following Su *et al.* (2, 3, 6), we adopt the model Hamiltonian

$$\mathcal{H} = -\sum_{n,s}[t_0 + (-1)^n\alpha(\psi_{n+1} + \psi_n)] \times [C^+_{n+1,s}C_{ns} + C^+_{ns}C_{n+1,s}] + \frac{K}{2}\sum_n(\psi_{n+1} + \psi_n)^2 + \frac{M}{2}\sum_n\dot{\psi}_n^2 - A[\psi_0 + (-1)^N\psi_{N-1}], \quad [1]$$

The publication costs of this article were defrayed in part by page charge payment. This article must therefore be hereby marked "*advertisement*" in accordance with 18 U. S. C. §1734 solely to indicate this fact.

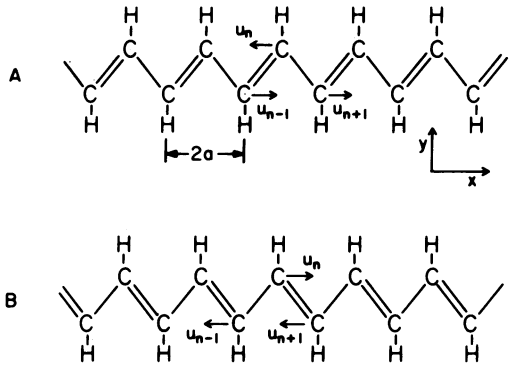

FIG. 1. Structure of the $(CH)_x$ chain, illustrating the pattern of displacement coordinates $\{u_n\}$ in the A (*Upper*) and B (*Lower*) phases.

to describe a chain of N groups, where K is the effective spring constant for the undimerized system, which is equal to 21 eV/Å^2 for $(CH)_x$, and M is the CH mass. The π band width is $4t_0 \simeq 10$ eV and the electron–phonon coupling is $\alpha \simeq 4.1$ eV/Å. The staggered displacement field ψ_n is related to the physical displacement u_n of the nth CH group along the symmetry axis (x) of the polymer by

$$\psi_n = (-1)^n u_n \quad [2]$$

as illustrated for the two degenerate classical ground states in Fig. 1 *Upper* ($\psi_n = -u_0$) and *Lower* ($\psi_n = u_0$), where $u_0 \approx 0.04$ Å. The parameter A is chosen such that $\psi_n = 0$ for all n corresponding to the ground state in the undimerized sector.

Adiabatic approximation

To integrate the equations of motion, we assume that the adiabatic (Born–Oppenheimer) approximation holds. As Brazovskii and Dzyaloskinskii (7) have shown, this approximation is justified if the Peierls gap 2Δ [$\approx$1.4 eV for $(CH)_x$] is large compared to the optical phonon energy $\hbar\omega_0 \approx 0.14$ eV. A restriction on their proof is that the magnitude of order parameter $|\psi|$ must not be reduced to a small fraction of its equilibrium value u_0 anywhere along the chain. Because we are interested in amplitude solitons in which ψ passes through zero at the soliton center, a more general justification of the adiabatic approximation is required. In conventional metals, the adiabatic approximation works well in treating lattice dynamics because the phase space for creating electron–hole pairs is very small at the low energies corresponding to phonon destruction. We argue that the same justification holds for $(CH)_x$, an assumption which can be checked self-consistently from the electron spectrum one obtains from the adiabatic approximation.

Within the adiabatic approximation, the coordinates $\{\psi_n\}$

* Permanent address: Department of Physics, University of Pennsylvania, Philadelphia, PA 19104.

move in a potential $V(\{\psi_n\})$ given by the sum of the ground state energy $E_0(\{\psi_n\})$ of the electronic system plus the harmonic lattice interaction in Eq. 1,

$$V(\{\psi_n\}) = E_0(\{\psi_n\}) + \frac{K}{2}\sum_n (\psi_{n+1} + \psi_n)^2 - A[\psi_0 + (-1)^N\psi_{N-1}]. \quad [3]$$

For given $\{\psi_n\}$, E_0 is the sum of the energies ϵ_v of the occupied one-electron energy eigenstate φ_v,

$$E_0(\{\psi_n\}) = \sum_{vs} \epsilon_v(\{\psi_n\})n_{vs}. \quad [4]$$

where n_{vs} is the occupation number of orbital v with spin orientation s. The total number of electrons is

$$n = \sum_{vs} n_{vs}. \quad [5]$$

The ϵ_v's are the eigenvalues of an effective one-electron Hamiltonian $\mathcal{H}$ whose matrix elements in the site representation are

$$\mathcal{H}_{nn'} = \begin{cases} -t_0 - (-1)^n\alpha(\psi_{n+1} + \psi_n) & n' = n + 1 \\ -t_0 + (-1)^n\alpha(\psi_n + \psi_{n-1}) & n' = n - 1 \\ 0 & \text{otherwise} \end{cases} \quad [6]$$

so that the eigenvalue equation for φ_{vn} is

$$[-t_0 - (-1)^n\alpha(\psi_{n+1} + \psi_n)]\varphi_{vn+1} + [-t_0 + (-1)^n\alpha(\psi_n + \psi_{n-1})]\varphi_{vn-1} = \epsilon_v\varphi_{nv}. \quad [7]$$

For numerical convenience, we consider a finite length chain having N CH groups. We find instructive results for N as small as 30. For N of this order, it is convenient to find the ϵ_v's by seeking zeros of the secular determinant,

$$D(\epsilon) = \det[\mathcal{H}_{n'n} - \epsilon\delta_{n',n}] = 0. \quad [8]$$

For an even number of electrons, one fills the $N/2$ lowest energy states with two electrons each and for an odd number of electrons adds the extra electron to the next higher state to obtain the electronic ground state energy $E_0(\{\psi_n\})$.

For simplicity, we assume that the CH groups are sufficiently massive that the ψ_n's and the velocities $w_n = \dot{\psi}_n$ can be treated as classical variables. Numerical estimates show that this is a reasonable starting approximation. The classical equations of motion are

$$\frac{d\psi_n}{dt} = w_n \quad [9]$$

$$M\frac{dw_n}{dt} = -\frac{\partial V}{\partial\psi_n} \equiv F_n. \quad [10]$$

The derivative of V with respect to ψ_n is calculated as

$$F_n = -\frac{\delta V}{\delta\psi_n} \quad [11]$$

for suitably small $\delta\psi_n$.

To integrate the equations of motion, the initial coordinates $\psi_n(0)$ and the staggered velocities $w_n(0)$ must be specified. Then, using time steps of length τ, one has the set of iterative equations

$$\begin{aligned} w_n(1) &= w_n(0) + \frac{F_n(0)}{M}\tau, \quad \psi_n(1) = \psi_n(0) + w_n(1)\tau, \\ w_n(2) &= w_n(1) + \frac{F_n(1)}{M}\tau, \quad \psi_n(2) = \psi_n(1) + w_n(2)\tau, \\ &\vdots \qquad\qquad \vdots \\ w_n(m) &= w_n(m-1) + \frac{F_n(m-1)}{M}\tau, \\ \psi_n(m) &= \psi_n(m-1) + w_n(m)\tau. \end{aligned} \quad [12]$$

In Eq. 12, time is expressed in units of τ and $F_n(m)$ denotes the force on group n as calculated from the order parameters evaluated at time $m\tau$. In order to facilitate the calculations, we have chosen the spring constant K so that the soliton width is reduced from $\ell = 7$ for $(CH)_x$ to $\ell = 2.75$. In this case, u_0 corresponds to $\approx$0.1 Å compared to 0.04 Å for $(CH)_x$. The time step size τ is chosen to be 1.25×10^{-15} sec compared to the period of the $k = 0$ optical phonon $2\pi/\omega_0 = 36 \times 10^{-15}$ sec, so that the configuration changes smoothly with respect to time. We measure ψ_n in Å units.

Results

To illustrate the richness of the nonlinear dynamics of this system, we consider three distinct initial configurations. In the first, the normalized order parameter is initially $\bar{\psi}_n(0) = 1$ for all sites in the chain with an odd number of sites, where $\bar{\psi}_n(t) \equiv \psi_n(t)/u_0$. The second example traces the dynamics of the system, following the initial creation of an electron–hole pair by a photon. Finally, the third example shows the time evolution of the lattice distortion following the injection of an electron at the conduction band edge with ψ_n initially equal to 1.

Example 1: End-Kink Generation. In Fig. 2 the normalized order parameter is plotted as a function of n for several different times starting from the initial condition $\bar{\psi}_n(0) = 1$ for all n. As was shown by one of us (6), the ground state of a chain with an odd number of sites has a soliton located near the center

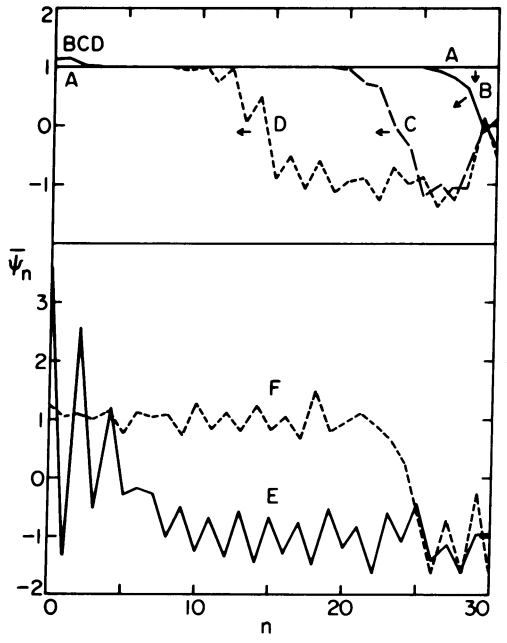

FIG. 2. Time evolution of $\bar{\psi}_n$, illustrating an end-generated soliton for time t = 0, 10, 40, 100, 226, and 400 in units of $\tau = 1.25 \times 10^{-15}$ sec.

of the chain. In chemical language, the initial state $\bar{\psi}_n(0) = 1$ corresponds to the chain ending in a double bond on the left and a single bond on the right. This is a high-energy state, and the system distorts to form a double bond at each end of the chain plus a soliton. As one sees from the plots, part of the energy lowering goes into phonons. For example, in curve D the rapid oscillations of the staggered order parameter $\bar{\psi}_n$ corresponds to large-amplitude long-wavelength acoustic phonons. Also, in curves B, C, and D, the order parameter at the left-hand end is increased above u_0 corresponding to an enhanced double bond strength at a free end. Curve E illustrates the soliton bouncing against the left-hand end of the chain and finally in curve F the soliton has moved back toward the right-hand end.

As in Fig. 3, if one plots the position of the center of the kink (i.e., the position where the interpolated value of $\bar{\psi}_n$ vanishes) as a function of time, one finds that the soliton's speed is essentially constant except when it is in contact with a chain end. The speed is found to be of order 1.3×10^6 cm/sec, which is close to the speed of sound in this model.

Example 2: $e + h \rightarrow S + \bar{S}$. Suppose that an electron–hole pair is suddenly created at time zero, with the electron at the bottom of the conduction band and the hole at the top of the valence band. We assume that at this instant the order parameter $\bar{\psi}$ is that for the ground state of the chain before the pair was created. The system is unstable in this electronically excited state and will evolve in time so as to create a soliton–antisoliton pair. The time evolution of $\bar{\psi}$ for this process is shown in Fig. 4. As one proceeds from curve A to B to C to D, the electron–hole pair continuously distorts the lattice, self-consistently localizing the electron–hole pair near the center of the chain in states split off from the conduction and valence band edges. As time progresses, phonons are generated as seen in curve E, and the soliton and antisoliton begin to separate. It is interesting to note that, according to this calculation, the time required to dress a bare electron–hole pair by forming a soliton–antisoliton pair is of order 10^{-13} sec rather than a long incubation time that one might guess based on the large change of the order parameter as well as the multiphonon generation which is observed.

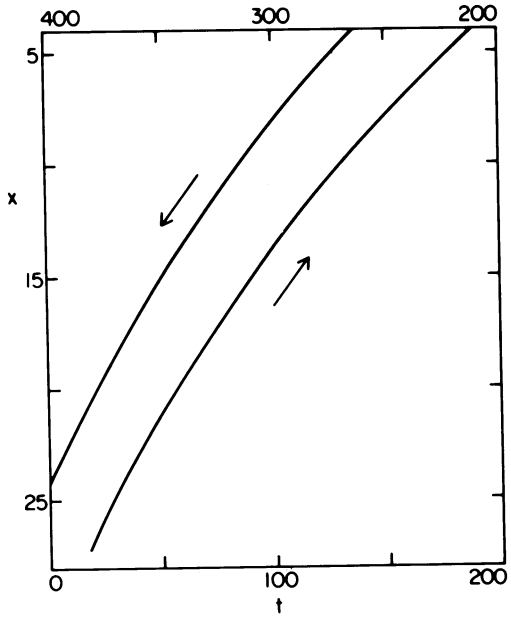

FIG. 3. Position of center of soliton in units of lattice spacing vs. time in units of $\tau = 1.25 \times 10^{-15}$ sec. The graph is folded in the time axis and illustrates the uniformity of the velocity.

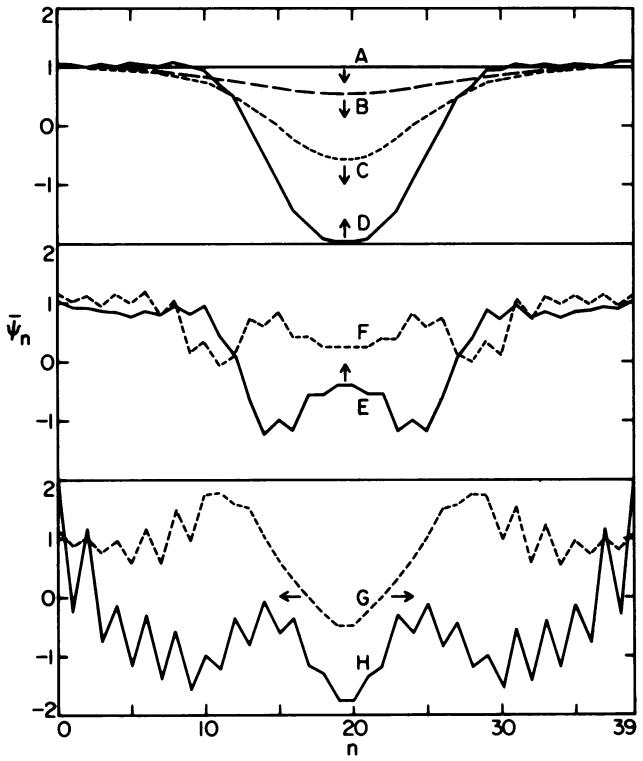

FIG. 4. $\bar{\psi}_n$ vs. n for $t = 0, 6, 12, 20, 30, 50, 60$, and 130 in units of $\tau = 1.25 \times 10^{-15}$ sec, describing the generation of a soliton–antisoliton pair from an electron–hole pair created at $t = 0$ at the band edges.

A matter of principle arises in the above discussion—namely, is it proper to consider that an electron–hole pair is created by photon absorption at an instant of time, even though the light intensity is weak so that the mean time to absorb a photon may be long compared to the relaxation time of 10^{-13} sec found above? The reason that the sudden creation picture is correct is familiar from the theory of measurement: precisely when the photon is absorbed is highly uncertain; however, when it *is* absorbed, the coupled electron–phonon system evolves in time as discussed above, even though we take the classical limit of

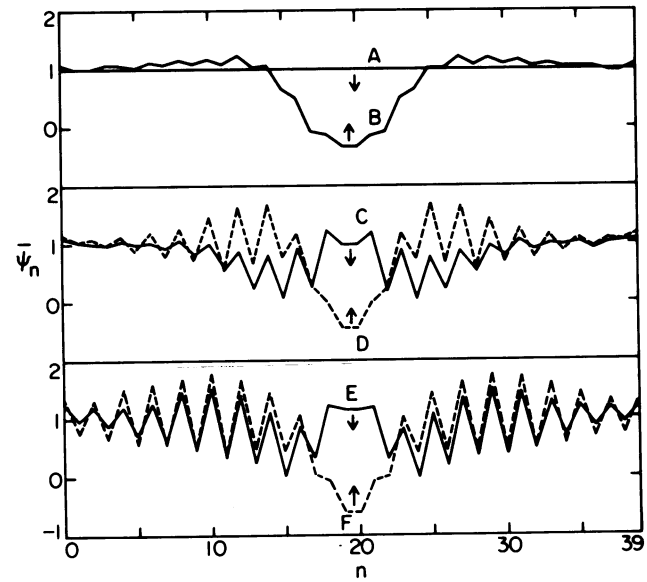

FIG. 5. $\bar{\psi}_n$ vs. n for $t = 0, 26, 50, 74, 96$, and 116 for $\tau = 1.25 \times 10^{-15}$ sec for an electron injected at the conduction band edge.

the lattice displacement equations of motion. Alternatively, treating both the electronic and lattice displacement coordinates quantum mechanically, the system's state vector Ψ, when acted upon by the electromagnetic potential $\vec{A}$ is given to first-order in $\vec{A}$ by

$$|\Psi(t)\rangle = e^{-iHt}\left[1 + \frac{i}{c}\int_0^t \vec{j}(t')\cdot\vec{A}(t')dt'\right]|\Psi(0)\rangle \quad [13]$$

where j is the total electric current and c is the speed of light. Thus, to first-order in $\vec{A}$, the time evolution of the component of $|\Psi(t)\rangle$ due to $A(t')dt'$ is unaffected by A at other times.

Example 3: Electron Injection. To investigate the dynamics of the system after the injection of an electron (or a hole)—e.g., in a tunneling experiment—consider placing an electron at the bottom of the conduction band at time zero, with $\bar{\psi}_n(0) = 1$ for all n. Fig. 5 illustrates how the electron self-consistently distorts the lattice and is localized in a split-off state, forming a "strong polaron." As time progresses, shake-off phonons appear, as evidenced by the large amplitude oscillations of $\bar{\psi}$ in curves C–F. In Fig. 6, the kinetic energy of lattice motion has been removed and the system is allowed to relax adiabatically to its ground state configuration in the presence of the added electron. This figure is analogous to the conventional picture of a strong polaron in a system without symmetry breaking. The binding energy of the polaron is ≈0.3 eV.

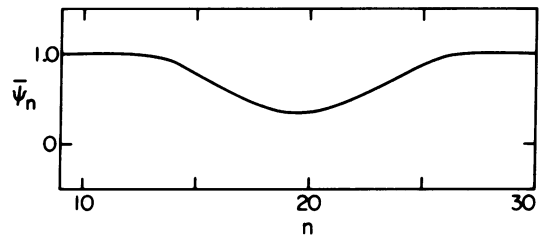

FIG. 6. $\bar{\psi}_n$ vs. n for the ground state of one electron added to the conduction band.

Discussion

The conventional picture of a rigid band semiconductor should be applied with care to polyacetylene, in which the gap parameter is determined self-consistently from the coupled electron–phonon system. For electron or hole injection as well as electron–hole pair creation, the order parameter distorts so rapidly that the electronic spectrum is significantly broadened. This distortion drastically alters the transport properties of electrons and holes because the excitations become charged solitons through this dressing process. One important result is that the charged solitons have a limiting velocity of approximately the speed of sound, which is very small compared to limiting velocities of electrons and holes in conventional semiconductors. Another is that the nonlinearity of the dynamics tends to suppress the recombination of soliton–antisoliton pairs.

We conclude that real time integration of the field equations is a powerful tool in studying various physical properties of the coupled electron-phonon system. The calculations are easily extended to include impurity effects.

The authors are grateful to Profs. A. J. Heeger and D. J. Scalapino for stimulating conversations. This work was supported in part by National Science Foundation Grant DMR 80-07432 and by the National Science Foundation MRL program at the University of Pennsylvania by Grant DMR 76-80994.

1. Peierls, R. E. (1955) *Quantum Theory of Solids* (Clarendon, Oxford).
2. Su, W. P., Schrieffer, J. R. & Heeger, A. J. (1979) *Phys. Rev. Lett.* **42**, 1698–1701.
3. Su, W. P., Schrieffer, J. R. & Heeger, A. J. (1980) *Phys. Rev.* **B22**, 2099–2111.
4. Ozaki, M., Peebles, D. L., Weinberger, B. R., Chiang, C. K., Gau, S. C., Heeger, A. J. & MacDiarmid, A. G. (1979) *Appl. Phys. Lett.* **35** (1), 83–85.
5. Rice, M. J. (1979) *Phys. Lett.* **71**, 152–154.
6. Su, W. P. (1980) *Solid State Commun.*, in press.
7. Brazovskii, S. A. & Dzyaloshinskii, I. E. (1976) *Zh. Exp. Tech. Fiz.* **71**, 2338.